Hysteresis of the stress-induced crystalline phase transition in poly(butylene terephthalate)

M. G. Brereton, G. R. Davies, R. Jakeways, T. Smith and I. M. Ward
Department of Physics, University of Leeds, Leeds 2, UK
(Received 2 August 1977)

The stress-induced crystalline phase transition in poly(butylene terephthalate), (4GT), has been investigated by X-ray diffraction and laser Raman spectroscopy. A well defined stress hysteresis effect has been demonstrated and a continuum theory has been developed which satisfactorily describes the temperature dependence of the phenomenon.

INTRODUCTION

Previous publications[1,2] have described how the main features of the mechanical behaviour of oriented poly(butylene terephthalate), (4GT), are strongly influenced by a change in the structure of the crystalline regions when the polymer is subjected to stress. By combination of X-ray diffraction and spectroscopic measurements it has been clearly established that the major effect is a change in the conformation of the glycol residue from the *gauche–trans–gauche* sequence in the unstressed state to the all *trans* sequence under stress. In the present paper this transformation is studied in greater detail over a wide temperature range, and particular attention is paid to the behaviour in loading and unloading cycles. Moreover, it is shown that the observed hysteresis in the crystal structure change can be understood in terms of a mean field model.

EXPERIMENTAL

Preparation of samples

The samples were prepared from 4GT polymer with a molecular weight characterized by a relative viscosity of 2.2, determined in a 1% solution in *o*-chlorophenol at 25°C. The polymer was extruded from the melt at 280°C through a rectangular die and immediately quenched into water. The resultant isotropic tape was drawn on a Meccano draw frame, over a heated roller (the pin) at 90°C and a heated plate at 160°C to a machine draw ratio of 5:1. The oriented tape was subsequently annealed at constant length under vacuum at 200°C for 20 h. This preparation procedure produced a tape of high orientation and crystallinity 1.2 mm wide and 20 μm thick.

X-ray measurements

X-ray measurements were made with a recording diffractometer using CuKα radiation produced by a Siemens K4 generator.

The specimens, which consisted of several tapes bunched together in order to increase the measured intensity, were mounted in specially designed extensometers attached to the independently rotating central turntable of the diffractometer and could be held either vertically, for recording equatorial reflections, or horizontally for making measurements on the near meridional reflections. The latter, the $\bar{1}04$ and $\bar{1}06$ reflections, were used to characterize the *c*-axis dimension of the unit cell since there is no true meridional reflection with measurable intensity available in the diffraction pattern.

An early check was made that the bundle of tapes behaved in the same way as a single tape and it was found that this was so, providing care was taken in fixing the ends in the extensometer clamps, there being no differential slipping. Diffraction patterns were recorded in the usual way by scanning the scintillation counter detector around in 2θ whilst the specimen rotated around in θ, i.e. at half the angular rate.

The intensity of a particular line was measured by recording the counting rate in the detector over a suitable time and subtracting the background count. It should be noted that the time response of the detecting system was such that a rough measure of intensity could be obtained in a second or so, although a longer counting time was normally used to obtain the experimental data described later.

The width at half height of a reflection was measured from the diffractometer scan. The instrumental width was around 0.2°–0.3°, hence the measured widths described later represent the natural widths of the reflections which we call $\Delta(2\theta)$. This quantity, measured in degrees, is related to the mean crystallite size, l_{hkl}, in a direction normal to the corresponding Bragg plane by the relation:

$$l_{hkl} = \frac{f\lambda}{\cos\theta \times \Delta(2\theta)}$$

where λ is the X-ray wavelength, θ is the Bragg angle and f is a constant close to unity (commonly taken as 0.9).

Crystal thicknesses in the *c*-axis direction, which very nearly coincides with the fibre axis, are estimated by multiplying l_{hkl} by $\cos\phi$ where ϕ is the angle between the plane normal and the *c*-axis. This assumption is justified by the nature of

Table 1 The angle, ϕ, between the normal to the specified Bragg planes and the *c*-axis direction

	Reflection	ϕ (degrees)
α Form	$\bar{1}04$	23
	$\bar{1}06$	12
β Form	$\bar{1}04$	12
	$\bar{1}06$	14

the lamellar structure which, as indicated by the small-angle X-ray scattering discussed in ref 1, is such that the lamellae are predominantly perpendicular to the fibre axis. The values of ϕ which were used are shown in *Table 1*.

Measurements of crystallite orientation were also carried out by holding the counter at the appropriate value of 2θ and rotating the specimen turntable. The resulting plot of count rate (corrected) *versus* the angle of rotation (ω) measured from the true Bragg position is a raw orientation curve. When the curve is corrected for geometrical effects it represents the angular distribution of crystallites in the sample and we characterize the degree of orientation in this work quite simply by means of the width at half height of the corrected orientation curve, $\Delta\omega$. The orientation curves that we measured assume true fibre symmetry in the specimens. Since tape specimens were produced there was some degree of biaxial orientation present which was not sufficient, however, to affect the interpretation of the orientation measurements (see below).

Measurements on the diffraction pattern at temperatures other than room temperature were accomplished by surrounding the specimen with a thin polyurethane foam enclosure through which cold nitrogen gas or hot air could be passed. The temperature of the specimen was measured by an adjacent thermocouple and stabilized by a temperature controller.

Raman spectroscopy

Raman spectroscopic measurements were made using a Coderg Pho double grating spectrometer, employing as an excitation source a 'Coherent Radiation' Argon ion laser, which produced about 10 mW of radiation at a wavelength of 488 nm.

Special apparatus was constructed to enable Raman measurements to be undertaken on the tape samples under stress over a wide range of temperatures (−100° to +150°C). Four thicknesses of the tape were mounted vertically in a small loading rig, enclosed in a double-walled brass container with optically flat, carefully aligned glass windows, so arranged as to permit both 90° and 180° scattering modes. The temperature of the enclosure containing the sample was measured with a thermocouple which was very close to the specimen but below the laser beam, to prevent specular reflections.

The experimental arrangements were such that a polarizer between the excitation source and the sample ensured that the input radiation was polarized either in a vertical plane parallel to the sample draw direction (described *V*) or in a horizontal plane perpendicular to the sample draw direction (*H*). There was a further polarizer (the analyser) which determined that the scattered radiation passing into the spectrometer was polarized either vertically (*V*) or horizontally (*H*).

Rectangular Cartesian axes 1, 2, 3 were chosen in the tape sample such that 3 is parallel to the draw direction and 1 is in the plane of the tape perpendicular to the draw direction. We introduce a simple notation for the scattered intensities, describing these by a matrix of scattered intensity components, I_{ij}, where i and j can take the values 1, 2, 3. This notation is such that, for example, in 90° scattering, if the input radiation is polarized vertically (in the 3 direction) and the scattered radiation is detected with the analyser horizontal (in the 1 direction) then the subsequent measured intensity is designated I_{13}. The intensity components for the different combinations of polarizer and analyser are shown in *Table 2*.

A particular intensity component will be affected in general by changes in molecular orientation as well as by changes in the concentration of the molecular species responsible for scattering. Bower[3] has shown how an invariant of the intensity components can be obtained whose magnitude relates only to the total number of scattering species. It may readily be shown that in our simplified notation, for a sample with transverse isotropy, this intensity invariant is given by $I_{inv} = 2I_{11} + I_{33} + 2I_{12} + 4I_{13}$.

A comprehensive study of the infra-red and Raman spectra of 4GT, including the changes occurring under stress, has recently been published[4]. The conclusion most relevant to the present investigation is that Raman lines associated with vibrations of the glycol residue show large changes in intensity with stress, whereas those associated with the terephthalate group show no significant changes in intensity, although there may be small shifts in frequency. In this work we report results based on the changes in intensity in the Raman line at 884 cm^{-1} which is assigned to an A_u CH_2 rocking mode of the *gauche–trans–gauche* conformation of the glycol residue. Because the absolute intensity of the scattered intensities may also change due to uncontrollable minor fluctuations in the experimental conditions we have used the 632 cm^{-1} line, which is assigned to a benzene ring B_{3g} C–C–C in-plane bending mode and shows no changes in either intensity or frequency with stress, as an internal standard. All the Raman data were therefore obtaintained in terms of the ratio of the values of I_{inv} as defined above, for the 884 cm^{-1} and 632 cm^{-1} lines. The measurements are complicated by the necessity to use both 90° and 180° scattering modes in order to obtain all four independent intensity components. Careful measurements on one sample showed that the absolute magnitudes of I_{33} and I_{13} determined from 90° and 180° scattering modes differed by less than 5%. Similar small differences were observed between the intensity components of the 632 cm^{-1} line for zero load and maximum load. It was therefore considered adequate to determine the relative scattered intensities for the 884 cm^{-1} and 632 cm^{-1} lines in each case and use these normalized scattered intensity components for the 884 cm^{-1} line to calculate a normalized I_{inv} which is a direct measure of the concentration of *gauche–trans–gauche* conformations.

Table 2 Polarization arrangements

	Polarizer	Analyser	Intensity
90° Scattering	*V*	*V*	I_{33}
	V	*H*	I_{13}
	H	*H*	I_{12}
180° Scattering	*V*	*V*	I_{33}
	H	*H*	I_{11}
	V	*H*	I_{13}

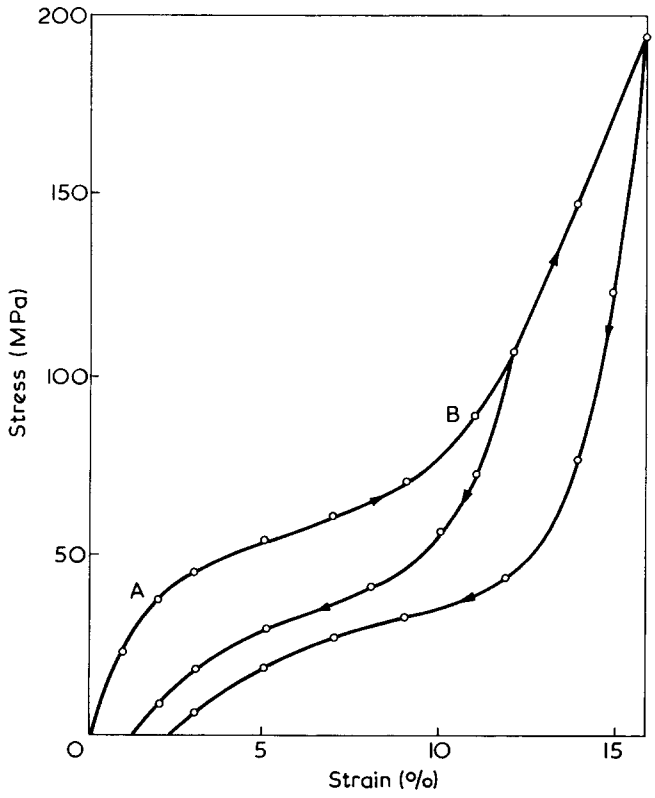

Figure 1 Typical relaxed stress–strain curves for an annealed 4GT tape. The arrows indicate whether stress is increasing or decreasing

RESULTS

Initial observations

In the preliminary investigations it was found that 4GT fibres displayed unusual mechanical properties at intermediate strains (~10%). A typical relaxed stress/strain curve *(Figure 1)* shows an initially steep rise of stress with strain (A) after which the stress rises much more slowly (A–B). Beyond B, which corresponds to a strain of about 12%, the stress again rises steeply with strain until failure occurs. A key observation is that although it might at first sight appear that the portion of the curve A–B corresponds to a region of plastic deformation, the strains induced in this region are recoverable as shown by the unloading curves from 12 and 15% maximum strain. X-ray diffraction measurements have shown[1] that the crystal structure of 4GT changes under stress from a 'relaxed' form, which we denote α, and in which the molecular chain is appreciably crumpled to a second form, which we denote β, in which the chain is essentially fully extended. This change in crystal structure is completely recoverable which thus accounts for the excellent strain recovery; the change in the molecular length in the crystal being about 12%.

Careful examination by X-ray diffractometry has shown[2] that at intermediate stress levels both crystal forms are present, the proportions changing from a just detectable presence of the β form at the point A to no detectable α form at the point B. Ref 2 showed how the intensity and Bragg angle of the $(\bar{1}04)$ and $(\bar{1}06)$ reflections of a drawn sample varied with stress at room temperature. The $(\bar{1}04)$ reflection was found to move discontinuously from a 2θ value of 31.4° to 27.8° (with CuKα radiation) whilst the $(\bar{1}06)$ moved from 47.9° to 43.0°.

Small changes (<0.5°) did take place in all four 2θ values while the stress level was being changed due to the elastic distortion of the crystalline lattice but there was no trace whatsoever of any reflections intermediate between those corresponding to the α form and those corresponding to the β form. As the α form reflection weakened in intensity, those from the β form strengthened. Equatorial reflections did not show a similar behaviour, but appeared to shift continuously by less than 1°. Whether this represents a continuous change in structure in this direction is a moot point since the reflections are intrinsically so broad (widths at half peak intensities of ~1°–2°) that any discrete change of Bragg angle of similar magnitude would appear to be continuous experimentally.

In addition to X-ray measurements, a detailed analysis of the changes in infra-red and Raman spectra has also been undertaken[4]. The results are consistent with two proposed structures of Hall and coworkers[5] where the extended form possesses an all *trans* CH_2 sequence in the glycol residue and the crumpled relaxed form is *gauche–trans–gauche.* These spectroscopic techniques have also been used as an independent method of monitoring the sample behaviour under stress.

This work attempts to examine more fully the temperature and time dependence of the above phenomena. The first observation was that the mechanical behaviour of a 4GT fibre specimen was strongly temperature dependent, and some relaxed stress/strain curves obtained by creep measurements or by an incremental strain programme on an Instron tensile testing machine are shown in *Figure 2.*

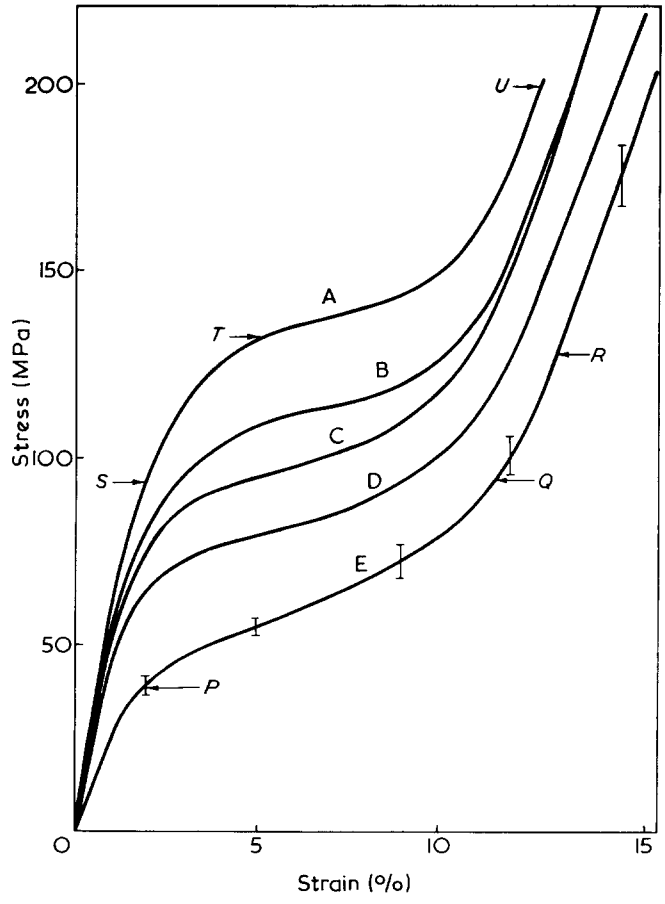

Figure 2 Relaxed stress–strain curves for annealed 4GT tapes taken at different temperatures. The 'stress increasing' portion only is shown. A, T = –91°C; B, T = –65°C; C, T = –45°C; D, T = –25°C; E, T = +22°C

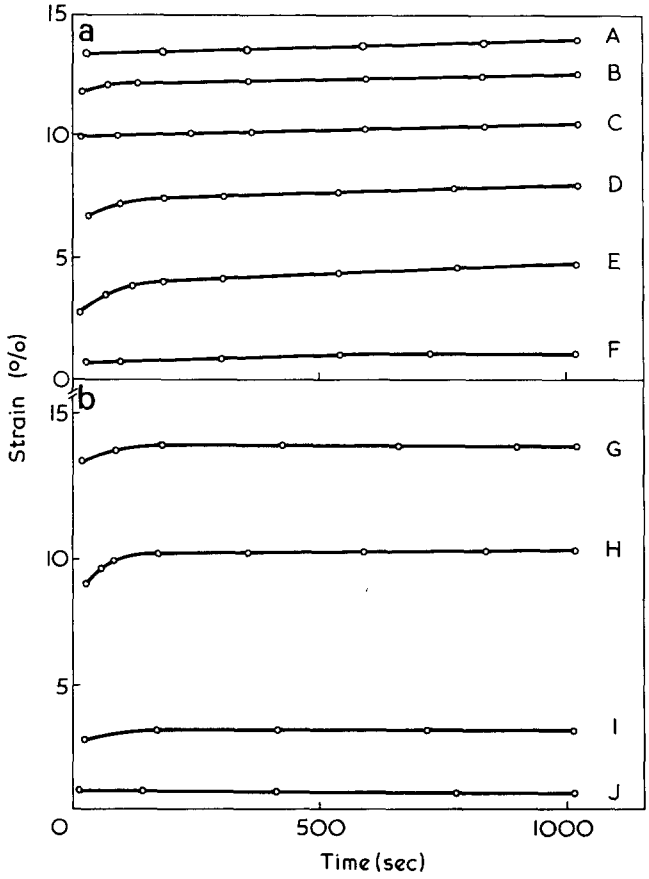

Figure 3 (a) The mechanical strain of a 4GT tape as a function of time with stress as a parameter at room temperature. (b) The same at a temperature of −88°C. Stress (MPa): A, 166; B, 119; C, 77; D, 60; E, 47; F, 24; G, 233; H, 150; I, 119; J, 49

No significant difference was found between the two methods and typical error bars are shown at various points on the room temperature curve. It is seen that the form of the curves is similar at all temperatures but that the stress required to maintain a constant strain increases as the temperature is reduced.

The time dependence of the crystal transition was studied by measuring the intensity of the $(\bar{1}06)$ reflection for either the α or β form as a function of time at a constant stress level chosen on the basis of the data shown in *Figure 2*. At room temperature the $(\bar{1}06)$ α form reflection was monitored at P and the $(\bar{1}06)$ β form reflection was monitored at both Q and R. Similarly, at −91°C the point S was used to monitor the α form and T and U to monitor the β form. At neither temperature did the intensity of the reflection change significantly with time indicating that there is no appreciable time dependence in the transition process.

In addition to these measurements the time dependence was further examined by measuring the creep strain of the bulk sample as a function of time for a range of stresses at different temperatures. Typical results are shown in *Figures 3a* and *3b*, for room temperature and −88°C respectively. These data clearly show that time dependent effects, though present, are typically small and limited to short times. As might be expected, any time dependent effects are greatest in the transformation region of the stress/strain curves, but even here they are relatively small.

The temperature dependence of the X-ray behaviour was initially explored by cooling a sample to −160°C and then applying a stress sufficient to give complete transformation to the extended β form at room temperature. It was found that the material remained in the α form for as long as it was convenient to maintain the low temperature, a period of 2–3 h. A similar experiment was performed in which the load was left on the sample whilst the temperature was raised in steps from −160°C to room temperature. Each intermediate temperature was maintained for 30 min during which the X-ray intensities were measured several times. These results are summarized in *Figure 4*. As the temperature was raised the transformation from the α to the β form progressed but there was no systematic time dependence at constant temperature.

To examine whether the behaviour depends upon the loading history a further experiment was conducted in which, between each step of increasing temperature, the specimen was raised to room temperature and the load was removed so that it reverted to the α form. The specimen was then cooled to the new low temperature and the load re-applied. The results of this experiment are also shown in *Figure 4* and it can be seen that the proportion of material transformed at any temperature was found to be very similar to that found in the first series of experiments. Again, no systematic time dependence was detectable in the X-ray measurements.

Phase transition hypothesis

It is seen from the initial observations described above that the transition from the α to the β form as detected by X-ray measurements is temperature dependent but not correspondingly time dependent as might be expected for a classical activated rate process. A simple theory was therefore devised which treats the $\alpha \rightarrow \beta$ transformation as a co-operative phase transition. The essential hypothesis of this theory is that the energy difference between the α and β forms at constant stress and temperature is not merely a

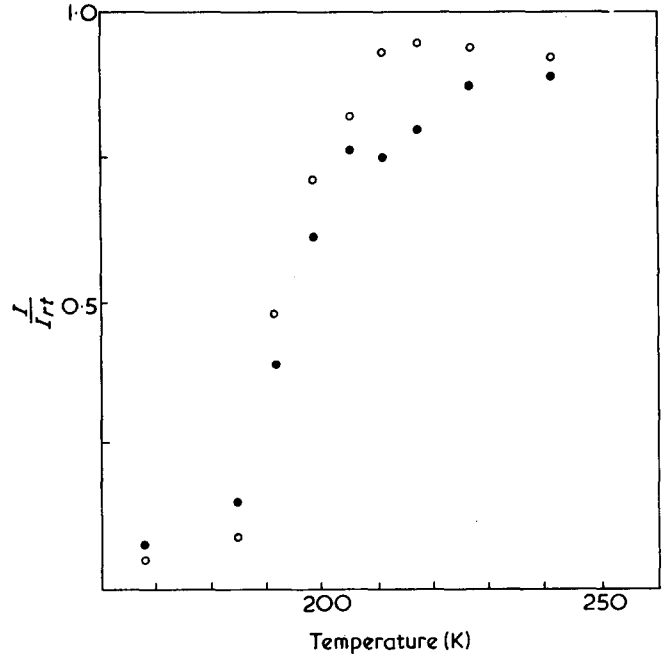

Figure 4 Normalized intensity of a β form X-ray reflection as a function of temperature at constant load. I, intensity at temperature indicated; I_{rt}, intensity at room temperature. ●, load maintained unchanged whilst temperature is increased in steps; ○, load removed and specimen heated to room temperature between each successive step (Only the data in the significant region of temperature are shown here)

constant but that it is dependent upon the relative amounts of α and β forms present at any time. Crudely speaking we are suggesting that it is 'easier' to produce more β form in a sample which already contains some β form than it is to produce it in a sample which consists entirely of the α form. The transition is therefore a cooperative phenomenon.

The theory is developed in terms of an order parameter m which describes the relative amounts of each crystalline form. If χ_β is the fraction of the sample in the extended β form and χ_α the fraction in the crumpled α form, then we define

$$m = \frac{\chi_\beta - \chi_\alpha}{\chi_\beta + \chi_\alpha} \tag{1}$$

When $m = +1$ the crystalline regions are entirely β form and when $m = -1$ they are entirely α form. There are various, and essentially equivalent, ways in which the order parameter may influence the free energy of the system. The approach we will adopt here is to use the idea of a local stress σ_L linearly dependent on m. In particular if σ is an applied tensile stress which favours the β form, then we take the local stress as

$$\sigma_L = \sigma + \kappa m \tag{2}$$

κ is an adjustable parameter which describes the strength of the cooperative interactions. We argue that since the β form is favoured by the applied stress, then the free energy per monomer unit for the conformation is lowered from G^o_β to G_β, where

$$\begin{aligned} G_\beta &= G^o_\beta - V_\beta \sigma_L \\ &= G^o_\beta - V_\beta \kappa m - V_\beta \sigma \end{aligned} \tag{3}$$

In these expressions V_β is a parameter with the dimensions of volume, and the free energy G^o_β is assumed to be a function of the temperature. Similarly, we argue that the free energy of the α conformation, which is not favoured by the applied stress, is raised from G^o_α to G_α, where

$$\begin{aligned} G_\alpha &= G^o_\alpha + V_\alpha \sigma_L \\ &= G^o_\alpha + V_\alpha \kappa m + V_\alpha \sigma \end{aligned} \tag{4}$$

Then the fraction of α and β forms at a temperature T and applied stress σ, is given by:

$$\frac{\chi_\beta}{\chi_\alpha} = \exp - \frac{(G_\beta - G_\alpha)}{kT} \tag{5}$$

If we define

$$\begin{aligned} 2G^o &= G^o_\beta - G^o_\alpha \\ 2V &= V_\beta + V_\alpha \\ kT_c &= \kappa V \end{aligned} \tag{6}$$

then

$$\frac{\chi_\beta}{\chi_\alpha} = \exp 2 \frac{(mkT_c - G_o + V\sigma)}{kT} \tag{7}$$

Using equations (1) and (7) the order parameter m is determined by the implicit equation

$$m = \tanh \frac{(mkT_c - G^o + V\sigma)}{kT} \tag{8}$$

The form of this equation is familiar from a wide variety of examples of phase transitions including magnetism[6]. At high enough temperatures with a stress applied there is only one stable value of the order parameter which corresponds to the extended β form. As the temperature is lowered two values of the order parameter are thermodynamically stable, corresponding to the extended β form or the crumpled α form. The state into which the system goes at this temperature now depends on the stress loading history and so there is a hysteresis effect. A detailed analytic discussion of the hysteresis is given in the Appendix.

Hysteresis investigations

The hysteresis experiments essentially consisted of measuring the amounts of α and/or β forms as a function of stress, following an increasing and then decreasing step loading sequence (i.e. the load was changed directly and very carefully from one level to another without allowing an intermediate zero load condition). Experimental quantities proportional to χ_α and χ_β, denoted f_α and f_β, were obtained by comparing the observed intensity $I(\sigma,T)$ of the $(\bar{1}06)$ reflection with the maximum value $I_{max}(T)$ obtained in the cycle thus:

$$f_\alpha = \frac{I_\alpha(\sigma,T)}{I_{\alpha max}(T)} \qquad f_\beta = \frac{I_\beta(\sigma,T)}{I_{\beta max}(T)}$$

At room temperature the normalization constant $I_{\alpha max}$ could be obtained from the zero stress data, it being assumed that under these conditions an insignificant amount of β phase was present. Likewise $I_{\beta max}$ could be obtained from the highest stress data assuming that very little α form was present. The quantity m was then calculated from:

$$m = \frac{f_\beta - f_\alpha}{f\beta + f_\alpha} \tag{10}$$

For most temperatures only $f\beta$ was measured and m was then calculated from:

$$m = 2f\beta - 1 \tag{11}$$

This procedure proved adequate at room temperature when samples of essentially entirely α or β form could easily be produced. At high temperatures, however, problems arose over the determination of $I_{\beta max}$ since the samples tended to break before complete transformation had been obtained, hence the highest observed value of I_β was used as an approximation of $I_{\beta max}$.

The results of a series of hysteresis experiments at different temperatures are shown in *Figures 5a–f*. The predicted hysteresis is clearly apparent, being most pronounced at low temperatures and tending to vanish at the highest temperatures. It is also seen that the general levels of stress rise as the temperature falls, in accordance with the mechanical data shown in *Figure 2*. As described in the Appendix,

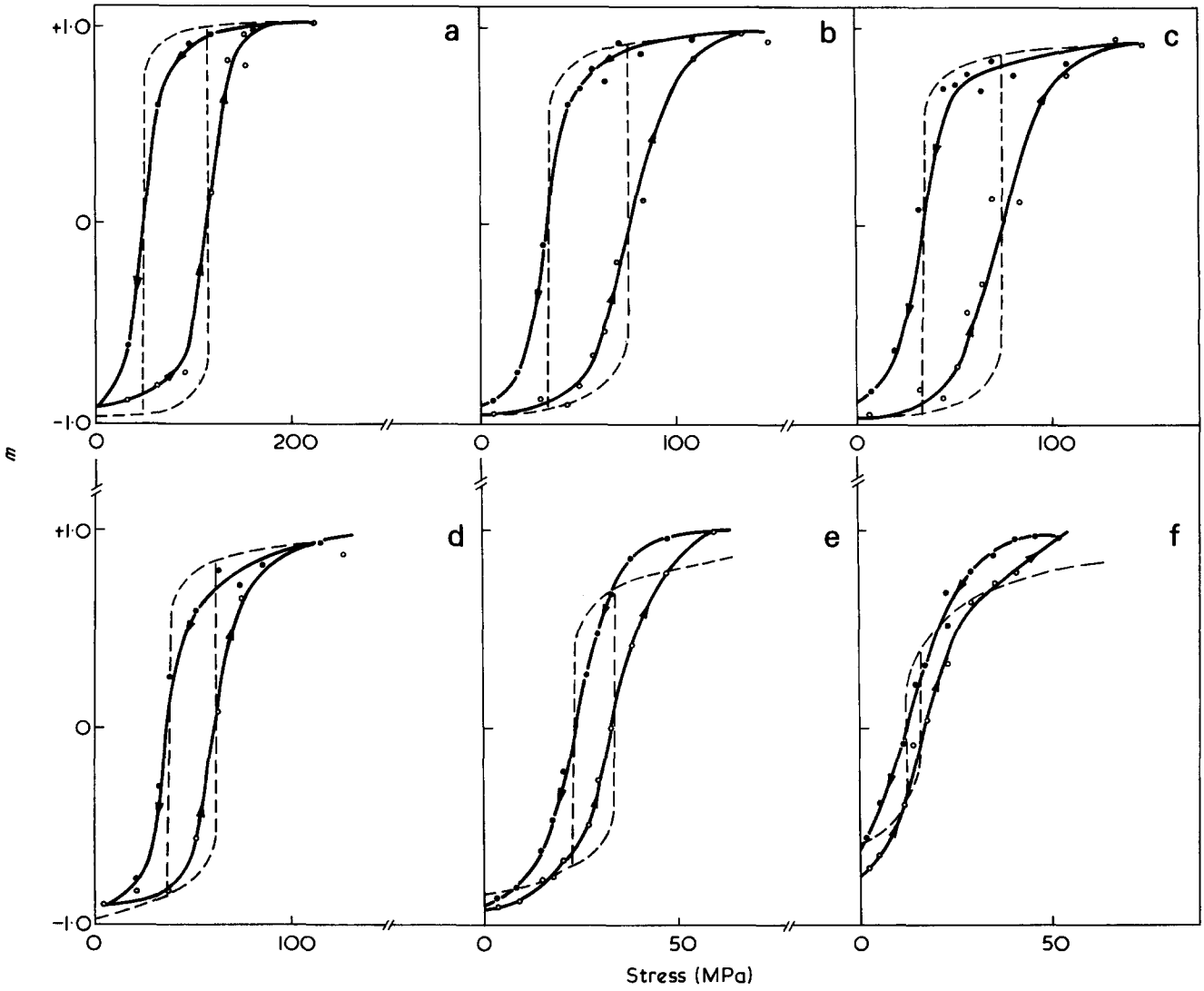

Figure 5 Experimental plots (——) of m deduced from X-ray data *versus* stress for stress increasing (○) and decreasing (●) at five different temperatures. (c) illustrates the effect of applying corrections to the data of (b) which are referred to in the text. The predictions of the theory are shown by the dotted lines. It should be noted that there are *three* different horizontal scales. (a) −24°C; (b) +23°C (raw data); (c) +23°C (corrected data); (d) +60°C; (e) +100°C; (f) +154°C

the width and position of the hysteresis loops provide the most convenient data for the determination of G°, V and T_c. Theoretical hysteresis curves obtained using these parameters are also shown in *Figures 5a–f*. It is seen that the general trend of the results is well represented by the theory but that the actual transition is not as sharp as is predicted. This is entirely analogous to the situation in ferromagnetism when experimental B–H loops are compared with a simple Weiss mean field model, and clearly indicates that detailed descriptions of the sample morphology are required for any more sophisticated theoretical treatment. One also observes that, at high temperatures and high stresses, the experimentally obtained values of m tend to be greater than the theoretically predicted values. This is a direct consequence of our inability to measure $I_{\beta max}$ accurately under these conditions.

In this semi-quantitative approach a variety of experimental complications have been ignored. As will be seen later the widths of the X-ray reflections changed with the application of stress and so did the degree of orientation of the crystallites. Furthermore, at the highest stresses employed bulk strains reached 15%, resulting in a significant thinning of the specimen.

Each of these effects leads to a (correctable) error in the assumed proportionality between the observed X-ray intensity and χ_α or χ_β. The curves of *Figure 5* have not been corrected but it turns out that such plots are relatively insensitive to small uncertainties in χ. This is illustrated in *Figure 5c*, which shows a fully corrected room temperature curve corresponding to *Figure 5b*. It is clear that any differences between the experimental curves are small in comparison with the discrepancies between theory and experiment.

Similar hysteresis experiments were performed using laser Raman spectroscopy. The results were worked out on the basis that the value of the normalized quantity I_{inv} at zero stress corresponds to 100% α form, i.e. $m = -1$. Measurements were undertaken at room temperature and −65°C and the data are shown in *Figure 6*. It can be seen that the results agree in form with the X-ray results in that hysteresis is observed at both temperatures and is much greater at −65°C. The Raman data however show that full transformation from the *gauche–trans–gauche* conformation to the all *trans* conformation is not achieved even at the highest stress levels employed. The room temperature Raman results also differ from the X-ray results on the loading cycle, in that the Raman data suggest that the transformation of

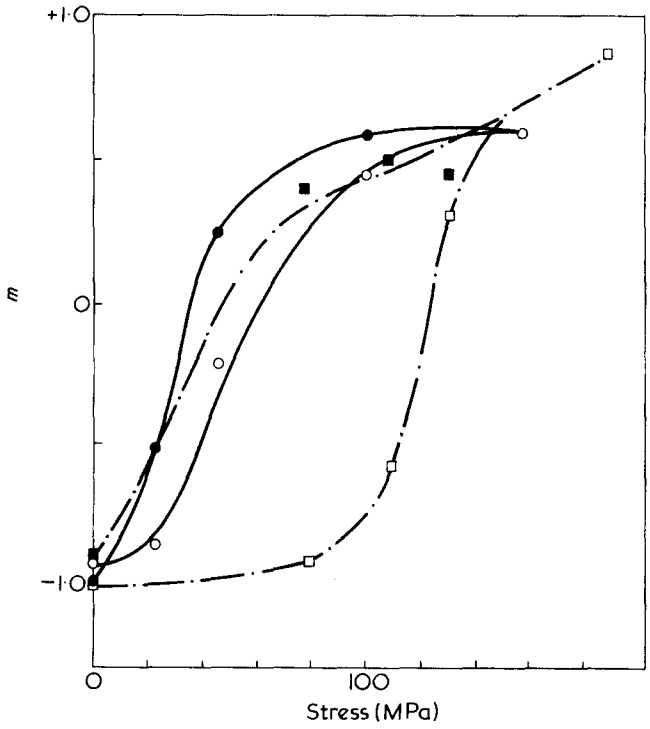

Figure 6 Experimental plots of m deduced from laser Raman observation at 884 cm^{-1} for stress increasing (○, □) and stress decreasing (●, ■) at two different temperatures. ○, ●, 20°C; □, ■, −65°C

material to the β form begins to occur at much lower stresses than shown by X-ray data.

Additional X-ray data–measurement of mean crystallite size and orientation

The phase transition hypothesis describes the experimental effects reported above but there still remains the problem of elucidating the mechanism by which the phase transition occurs. To this end further X-ray measurements were made of mean crystallite size and orientation in order to learn something of the changes in morphology that occur at the 'hundred angstrom' level which might give a clue to the nature of the transition.

First, the data of *Figure 7* which show the observed linewidths as a function of stress indicate that as the stress increases, the mean crystallite thickness in the chain direction of the α form decreases from 62 to 53 Å whereas the crystallites in the β form first appear with a mean thickness of 52 Å which steadily increases to around 75 Å. The uncertainties in these numbers are of the order of 5 to 10 Å and there is also present a degree of hysteresis as one might expect from the earlier measurements. Secondly, the data of *Figure 8* show that the degree of orientation, characterized by the value of $\Delta\omega$, remains substantially unchanged for the α form as the transition progresses. The β form crystallites, however, first appear with a greater value of $\Delta\omega$, i.e. they are *less* well oriented than the α form, and, as the transition progresses, the degree of orientation increases but never quite reaches the value for the α form.

Figure 9 shows the results of a comparison of the mean crystalline lattice strain with the overall sample strain. The mean lattice strain is simply the actual lattice strain which occurs when a molecule undergoes the transition multiplied by the fraction of ordered material which has transformed. There is a good deal of scatter in the points but there is a reasonably clear suggestion that the initial slope is less than 0.5 whereas the later slope is closer to 1.

This implies that, for low values of applied strain, the disordered material plays the greater role, there being a comparatively small degree of extension in the ordered, or crystalline, fraction.

DISCUSSION

The new aspect of behaviour reported in this paper is a well defined temperature-dependent hysteresis between the amount of a given crystal phase and the applied stress. Though the mean field theory accounts for this hysteresis and its temperature dependence it is an open question as to what the parameters T_c and V represent. At one extreme, T_c may be seen as representing the strength of the short range steric interactions between the molecules which favours neighbouring molecules having similar conformations in much the same way as the ferromagnetic Curie

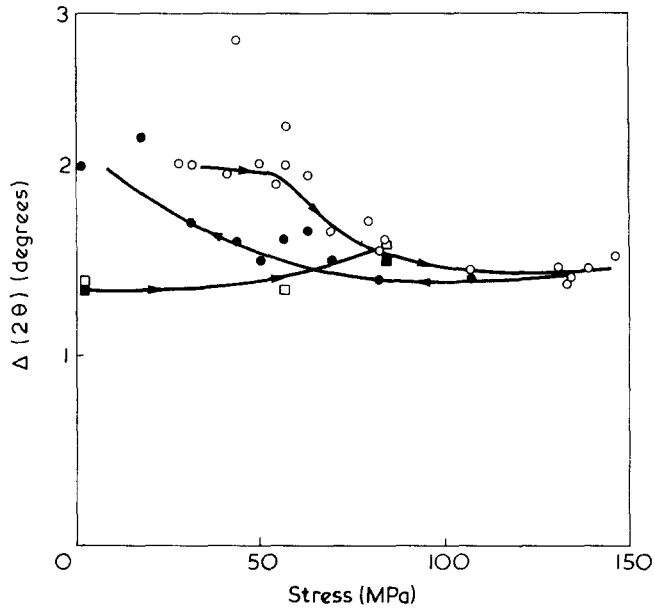

Figure 7 The full widths at half height of the 104 and 106 X-ray reflections from a 4GT tape specimen as a function of stress. □, $\bar{1}04$ α form, stress increasing; ■, $\bar{1}06$ α form, stress increasing; ○, $\bar{1}06$ β form, stress increasing; ●, $\bar{1}06$ β form, stress decreasing

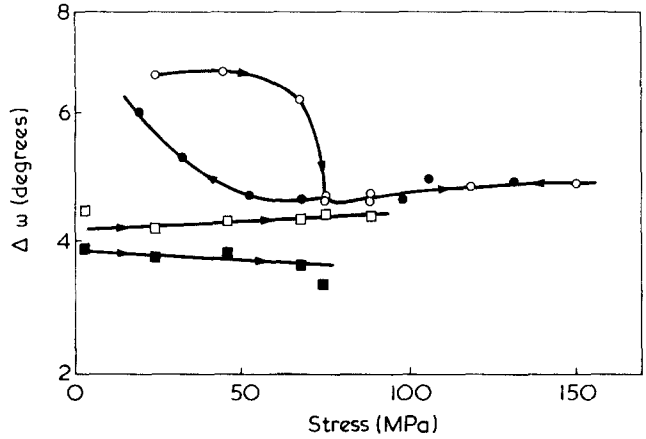

Figure 8 The full width at half height of the orientation curves as a function of stress. Key as *Figure 7*

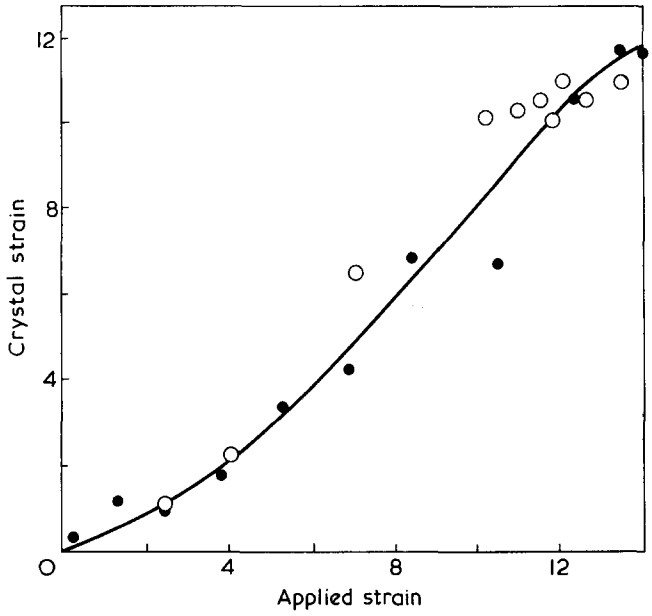

Figure 9 Mean lattice (crystal) strain *versus* applied sample strain measured at 23°C. ○, stress increasing; ●, stress decreasing

temperature represents the short range correlation between electron spins. At the other, a mathematically identical theory has been formulated in terms of a local stress σ_L related to the applied stress σ by:

$$\sigma_L = \sigma + \kappa m$$

The parameter, κ, which determines T_c, then describes the stress concentrating effect which the lengthening of a given unit has upon a neighbouring unit.

The physics of the nature of the cooperative interaction is thus very much an open question which requires further investigation since it clearly depends fundamentally upon the interaction between adjacent molecules or molecular chains about which there is at present no information. The detailed microscopic behaviour of the material when placed under stress should provide some useful pointers, however, and the additional X-ray measurements described above in conjunction with the Raman measurements enable us to draw several useful conclusions concerning the morphological changes which occur during the stretching process.

The marked increase in the mean length of the β form crystallites as the transition progresses suggest any, or all, of three possibilities. The first is that a boundary between the α and β form may be generated in an individual crystallite. This moves as stress increases but its position is not time dependent at constant stress. We have to assume further that, in the initial stages, only a few crystallites start to transform leaving the mean length of the α units substantially unchanged. The slight decrease in the latter quantity strengthens this hypothesis but the evidence is not totally convincing.

The second possibility is that, in the vicinity of very small crystallites, local stress variations are of greater magnitude than around larger crystallites and such crystallites may transform first.

Yet a third possibility is that of stress crystallization of small regions of the disordered material directly into the β form. The orientation data show that the initially transformed material is less well oriented than the crystalline fraction in the relaxed room temperature state, and it is quite plausible to suppose that the disordered material is, on average, less well oriented than the crystalline fraction.

The Raman data lend further supporting evidence and also give us an insight into the conformations of isolated molecules which are not detected using X-ray scattering. For example, it is found that the Raman bands corresponding to the α form tend to be comparatively narrow and to remain so at all values of stress. The β form bands on the other hand are always broad. These observations suggest that the α form only exists in an ordered or crystalline configuration but that individual molecules in the disordered material take the β form under stress and local stress variations lead to band broadening.

Thus, whereas the 4GT molecule exhibits two distinct stable, or metastable forms when in a crystalline environment, it would appear that an isolated molecule can take up a whole range or configurations when it is free but when it is placed under tensile stress it tends to adopt the β or all *trans* form.

Finally, consideration of *Figure 9* in which mean strain in the crystalline regions is compared with the macroscopically applied strain shows in particular that, in the transformation region (from about 4 to 11% applied strain) the incremental crystal strain and applied strain are equal. This is reminiscent of ideal plastic behaviour and suggests that once the mean strain in the material is sufficient to initiate the transformation process the degree of transformation is determined solely by geometric considerations, i.e. the overall deformation of the sample.

CONCLUSION

An unusual crystalline phase transition has been described which shows, in contradistinction to many other properties of polymers, no time dependence. A macroscopic theoretical description involving a cooperative transition phenomenon appears to describe the temperature dependence of the transition process reasonably well. There is, at present, no microscopic theory which offers a similar description but it is hoped that further detailed structure measurements will lead to such a theory.

REFERENCES

1 Jakeways, R., Ward, I. M., Wilding, M. A., Hall, I. H., Desborough, I. J. and Pass, M. G. *J. Polym. Sci. (Polym. Phys. Edn)* 1975, **13**, 799
2 Jakeways, R., Smith, T., Ward, I. M. and Wilding, M. A. *J. Polym. Sci. (Polym. Lett. Edn)* 1976, **14**, 41
3 Bower, D. I. *J. Polym. Sci. (Polym. Phys. Edn)* 1972, **10**, 2135
4 Ward, I. M. and Wilding, M. A. *Polymer* 1977, **18**, 327
5 Desborough, I. J. and Hall, I. H. *Polymer* 1977, **18**, 825
6 Weiss, P. *J. Phys. (Paris)* 1907, **6**, 661

APPENDIX

We require to solve the following equation relating m, T and σ:

$$m = \tanh\left(\frac{mkT_c - G^o + V\sigma}{kT}\right) \quad \text{(A1)}$$

The solution of this equation is readily demonstrated by graphical techniques. We define the variable θ such that:

$$m = \tanh(\theta) \quad \text{(A2)}$$

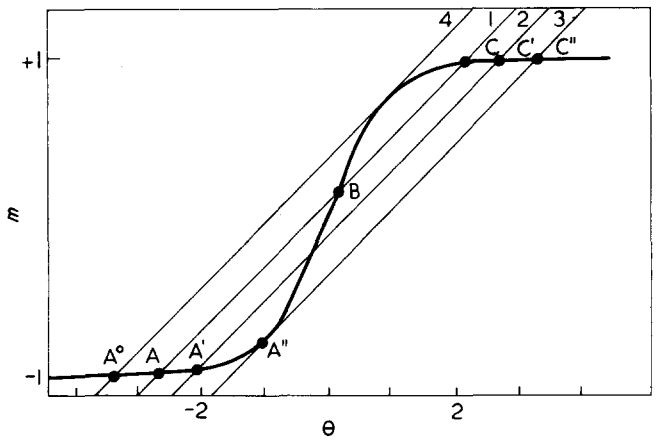

Figure A1 Plots of m *versus* θ deduced from equations (A2) and (A4). It should be noted that θ is a dummy variable having no direct physical significance and that values of m of +1 and −1 correspond to 100% β form and 100% α form, respectively

$$\theta = (mkT_c - G^o + V\sigma)/kT \tag{A3}$$

or, more conveniently for our purposes:

$$m = \frac{T}{T_c} \times \theta + \left(\frac{G^o - V\sigma}{kT_c}\right) \tag{A4}$$

If equations (A2) and (A4) are plotted, as shown if *Figure A1*, then the intersections of the straight line [equation (A4)] and the tanh curve are unity and for $T > T_c$ the slope of the straight line is greater than unity. Therefore, for temperatures above T_c there is only one point of intersection between the line and the curve and hence a unique solution for m.

For temperatures $T < T_c$, however, three possible values for m may be found as shown by the points A, B, and C on line 1 in *Figure A1*. The middle solution B corresponds to a local energy maximum and there are therefore only two stable solutions for m indicated by the points A and C. Which of these two solutions should be chosen to represent the state of the system depends upon its mechanical and thermal history. In particular, the system exhibits stress hysteresis as will now be demonstrated.

Suppose that the system is in state A on line 1, this being a typical low stress state for a room temperature experiment. As the stress is increased the tanh curve and the slope of the straight line remain unchanged but the intercept of the straight line on the m-axis is moved to an algebraically smaller value as indicated by line 2. The new solution for m, indicated by A', is less negative than A thus describing the increase in β phase content produced by the stress. It is apparent that with further increase in stress, m increases more rapidly thus leading to the upward curve on the low stress portion of the theoretical hysteresis curves shown in *Figure 5*. There comes a point, however, when a critical stress is reached as indicated by line 3. The solution point A'' represents the point where the straight line is tangential to the tanh curve, thus an infinitesimal increase in stress causes this solution to disappear, leaving only the solution point C''. The system therefore undergoes a rapid increase in β phase content, indicated by the vertical line in the theoretical hysteresis curves, as it attains the solution point C''. Further increase in stress can now only produce relatively small changes in m. If the stress is progressively reduced from this high value we can return to the stress level indicated by line 1 but the system is now represented by the solution point C and not A. To return to the latter point requires a further reduction in stress as indicated by line 4 which again represents a critical tangent condition where the system now makes a rapid transition to the point Å. Increase in stress then returns the system to the point A.

It is apparent that, for a variety of reasons, the experimental hysteresis curves do not show the sharp vertical transitions indicated by this simple theory. There is, however, a striking correlation between the theoretical and experimental curves when one considers the change in width of the curves as a function of temperature. This is such a pronounced effect that three different scales are used in *Figure 5*, to show the curves at different temperatures in reasonable detail. We have therefore used the width of the hysteresis curves (on the stress axis) as the means of estimating the parameters V and T_c.

We refer to the values of m and σ at the points where the straight line and the tanh curve are tangential as 'critical values' and denote them as m_c and σ_c respectively.

Equating the gradients of equations (A2) and (A4) we obtain:

$$\text{sech}^2(\theta) = \frac{T}{T_c} \tag{A5}$$

But

$$\text{sech}^2(\theta) = 1 - \tanh^2(\theta) \tag{A6}$$

$$= 1 - m_c^2 \tag{A7}$$

Hence

$$m_c = \pm(1 - T/T_c)^{1/2} \tag{A8}$$

The quantity m_c is not easy to estimate from the experimental data, but using equations (A8) and (A1) we may obtain:

$$\sigma_c = \frac{kT}{2V} \ln\left(\frac{1 + m_c}{1 - m_c}\right) - \frac{m_c kT_c}{V} + \frac{G^o}{V} \tag{A9}$$

There are two values of σ_c corresponding to the positive and negative values of m_c respectively.

Denoting these by σ_c^+ and σ_c^- we obtain the width of the hysteresis loop, $\Delta\sigma$.

$$\Delta\sigma = \sigma_c^+ - \sigma_c^- = \frac{kT}{V} \ln\left(\frac{1 + m_c}{1 - m_c}\right) - \frac{2m_c kT_c}{V} \tag{A10}$$

In the above equation, m_c is to be regarded as a positive quantity. Now for a given T and $\Delta\sigma$ equations (A8) and (A10) define a relationship between V and T_c and it is not possible to determine values for either of these quantities from the width of any *one* hysteresis loop.

If, however, we plot V vs. T_c separately for each experimental hysteresis loop we obtain a set of curves all of which cross in the neighbourhood of $V = 40$ Å^3 and $T_c = 167$°C (440K). A plot of $\Delta\sigma$ *versus* T also extrapolates to zero width in the neighbourhood of 167°C hence we feel justified in adopting this as the best value of T_c, although

there is no obvious physical interpretation of this temperature.

The value of 40 Å^3 deduced for V is of similar magnitude to the change in volume of the unit cell in the transition which has a value of around 10 Å^3.

To deduce a value for G^o we observe that the midpoint of a hysteresis loop occurs at a value of σ given by:

$$\bar{\sigma} = \frac{\sigma^+ + \sigma^-}{2} = \frac{G^o}{V} \quad \text{(A11)}$$

G_o is then found to range from 20 meV at −24°C to 3.4 meV at +154°C.

The theoretical hysteresis loops of *Figure 5* were then calculated using the three parameters determined as described above.